Australian Government
Bureau of Meteorology

Improved tropical cyclone forecasts with CoMorph-A: Physical insights from TC-Kirrily

Hongyan Zhu, Debra Hudson, Sally Lavender

March 2026

Bureau Research Report - 123

Improved tropical cyclone forecasts with CoMorph-A: Physical insights from TC-Kirrily

Hongyan Zhu[1], Debra Hudson[1] and Sally Lavender[2,3]

[1]Bureau of Meteorology, Australia

[2]Centre for Applied Climate Sciences, University of Southern Queensland, Australia

[3]Met Office, United Kingdom

Bureau Research Report No. 123

March 2026

National Library of Australia Cataloguing-in-Publication entry

Authors: Hongyan Zhu, Debra Hudson, Sally Lavender

Title: Improved tropical cyclone forecasts with CoMorph-A: Physical insights from TC-Kirrily

ISBN: 978-1-923469-17-4

ISSN: 2206-3366

Series: Bureau Research Report – BRR123

Enquiries should be addressed to:

Corresponding Author: Hongyan Zhu

Bureau of Meteorology

GPO Box 1289, Melbourne

Victoria 3001, Australia

hongyan.zhu@bom.gov.au

Copyright and Disclaimer

Contents

List of Figures:

Executive Summary

Tropical cyclone (TC) Kirrily caused widespread damage and flooding across western Queensland in January 2024. This study evaluates forecasts of TC Kirrily using the Unified Model configurations GA8GL9 and GAL9, run with both the default convection scheme and the CoMorph-A convection scheme. CoMorph-A comprises the CoMorph convection scheme along with a suite of updates to physical parameterisations that interact with convection – specifically the boundary layer, microphysics and prognostic cloud schemes. The GAL9 configuration includes significant changes to most parts of the model physics including updates to the convection scheme. Forecasts using the default convection scheme in both GA8GL9 and GAL9 struggled to capture the cyclone's rapid intensification, resulting in underestimation of storm intensity. GAL9 showed marginal improvement over GA8GL9, but both remained weaker than observed. In contrast, GA8GL9 and GAL9 using CoMorph-A demonstrated a significant improvement, better replicating Kirrily's evolution, although somewhat over-deepening the TC. A key distinction in the results using the two different convection schemes is in the representation of convective–large-scale rainfall coupling. The default model configurations captured the dominance of parameterized convection during the developing stage of the TC, but they failed to transition to large-scale rainfall as the cyclone matured. CoMorph-A successfully represented this transition in the inner core, where deep convection shifted from being primarily parameterized to increasingly driven by large-scale moist processes. This shift facilitated rapid intensification and sustained cyclone strength, highlighting the importance of accurately modelling moisture processes in tropical cyclones.

1. Introduction

Tropical cyclones (TCs) are among the most powerful and destructive weather systems, posing significant threats to life, infrastructure, and economies. Accurate simulation and prediction of these storms are essential for effective disaster preparedness and mitigation. Numerical weather prediction (NWP) models play a crucial role in forecasting TCs, and one of the key components influencing their accuracy is the representation of convection.

Convection parameterization schemes are designed to approximate the effects of sub-grid scale convective processes that cannot be explicitly resolved by model grids (Arakawa A. 2004, Betts 2004). The choice of convection scheme significantly affects the simulation of TC formation, length of the gestation period, intensification, and structure (Zhu et al. 2001, Ma and Tan 2009, Shen et al. 2019, Smith 2000, Shepherd and Walsh 2016).

In this study, we use the Unified Model (UM) GA8GL9 (Global Atmosphere version 8 and Global Land version 9; Willett et al., 2025) and the newly developed GAL9 (Global Atmosphere and Land version 9; Xavier et al., 2023) model configurations. GA8GL9 is the model configuration of the Australian Bureau of Meteorology's operational global NWP system (Zidikheri et al., 2024) and is the atmosphere-land component in the Met Office's operational coupled model NWP system. Both GA8GL9 and GAL9 use the 6A mass flux convection scheme, based on Gregory and Rowntree (1990). This scheme often struggles to accurately capture the interaction between convective and large-scale moisture processes (Lock et al., 2024). The Met Office have been developing a new convection scheme, called CoMorph (Whitall and Matsubayashi, 2022; Lavender et al., 2024, Daleu et al., 2023, Lock et al., 2024, Zhu et al., 2024), which aims to model moisture process representation by improving the coupling between convection and resolved dynamics. In this study, we investigate the impact of the two different convection schemes on the simulation of TC Kirrily, which formed on 17 January 2024 and intensified to a Category 3 cyclone before weakening post-landfall over western Queensland. We compare forecasts using the default 6A convection scheme with those using the CoMorph-A package, which includes the CoMorph convection scheme and associated physical parameterisation updates. The analysis focuses on each configuration's ability to capture Kirrily’s intensity evolution, track, and rainfall characteristics. The findings contribute to the ongoing development of improved NWP models, ultimately enhancing the accuracy of TC forecasts and supporting more effective disaster risk management.

The paper is organized as follows: Section 2 describes the models and convection schemes. Section 3 describes the large-scale environment of TC Kirrily. The results are discussed in Section 4, followed by the conclusion in Section 5.

2. Model description

In this study, we employ the latest scientific configurations of the Met Office atmospheric models. Specifically, we use GA8GL9, which combines the Global Atmosphere model version 8 (GA8) with the JULES Global Land surface model version 9.0 (GL9) (Willett et al., 2025). Building upon this, we also utilize GAL9 (GA9GL9), a more recent configuration that incorporates several developments in model physics—most notably, enhancements to aspects of the convection scheme and associated parameterisations (Xavier et al., 2023). Both GA8 and GA9 use the same convection scheme, described in Section 2.1.1 below. However, GA9 incorporates additional modifications to most areas of model physics, including a few developments included in the CoMorph package.

The horizontal grid spacing used in this study is ~12km (N1024) with 70 levels in the vertical with its model top at approximately 80 km.

This is the resolution used in the Bureau of Meteorology's deterministic global forecast system, ACCESS-G4 (Zidikheri et al., 2024).

2.1. Convection schemes

The mass-flux convection scheme in the UM diagnoses conditions suitable for convection using an undiluted parcel ascent from near the surface (Gregory and Rowntree, 1990). For deep convection, the cloud-base mass-flux is calculated by reducing Convectively Available Potential Energy (CAPE) to zero over a given timescale (Gregory and Rowntree, 1990). The UM, like many models, has struggled with coupling convection and model dynamics, impacting phenomena such as the MJO and equatorial waves.

To address these issues, a new convection scheme called CoMorph is being developed (Whitall et al., 2022; Lock et al., 2024; Lavender et al., 2024; Zhu et al., 2024). CoMorph-A is the first release of a package of changes, including the CoMorph convection scheme, which aims to improve the coupling between convection and resolved dynamics. Tests have shown promising results, such as in the Indo-Pacific and Australian regions (Zhu et al., 2024).

2.1.1. The 6A convection scheme

In GA8 and GAL9, the default convection scheme is the 6A mass flux scheme of Gregory and Rowntree (1990). The 6A convection scheme defines the following types of convection:

- Shallow convection starting from the boundary layer and stopping below the freezing level or below an inversion with descent or weak ascent above. The shallow mass flux scheme was developed to model oceanic shallow convection like that observed by the BOMEX3 campaign (Holland 1970).

- Deep convection starting from the boundary layer and not diagnosed as shallow convection.
- Mid-level convection starting above the boundary layer or above shallow or deep convection. In the UM this can represent convection in mid-latitude storms, nocturnal convection over land and small-scale instabilities over a few model levels (i.e. numerical noise).

Further details of the convection scheme in GA8 are discussed in Willett et. al. (2025).

GAL9 builds on GA8GL9 with improvements to components of the 6A convection scheme, including:

- Alignment of mid-level and deep convection, in which mid-level convection is modified such that the differences between it and deep convection are reduced. Deep convection is then switched off.
- Modification of the CAPE calculation to include forced detrainment weighted CAPE. This has the advantage of making the closure more sensitive to low-level inversions.

2.1.2. CoMorph-A configuration

CoMorph is also a mass-flux convection scheme (Whitall and Matsubayashi, 2022). CoMorph features a new code structure for greater flexibility and includes additional physical processes. It initiates mass flux based on local instability and scales entrainment with parcel radius. CoMorph also includes a novel in-parcel parameterised bulk microphysics scheme for hydrometeor generation, which integrates with the model's grid-scale microphysics. This scheme allows for more accurate representation of precipitation and cloud processes, including graupel. CoMorph uses mixing ratios for water vapor and condensate, improving consistency and reducing global water conservation errors.

CoMorph-A is the first release of a package of changes that includes CoMorph in addition to modifications to the boundary layer, large-scale microphysics and prognostic cloud schemes which closely interact with the convection scheme (Whitall et al. 2022, Lock et al. 2024, Lavender et al. 2024, and Zhu et al. 2024). This is the first version of a scheme that is still being substantially developed.

Hereafter, the default atmosphere model configurations, GA8GL9 and GAL9 which use the 6A convection scheme, will simply be referred to as GA8 and GA9 respectively. When the CoMorph-A convection package is used instead, the configurations will be referred to as GA8-CoM and GA9-CoM.

3. **Large scale environment of TC Kirrily**

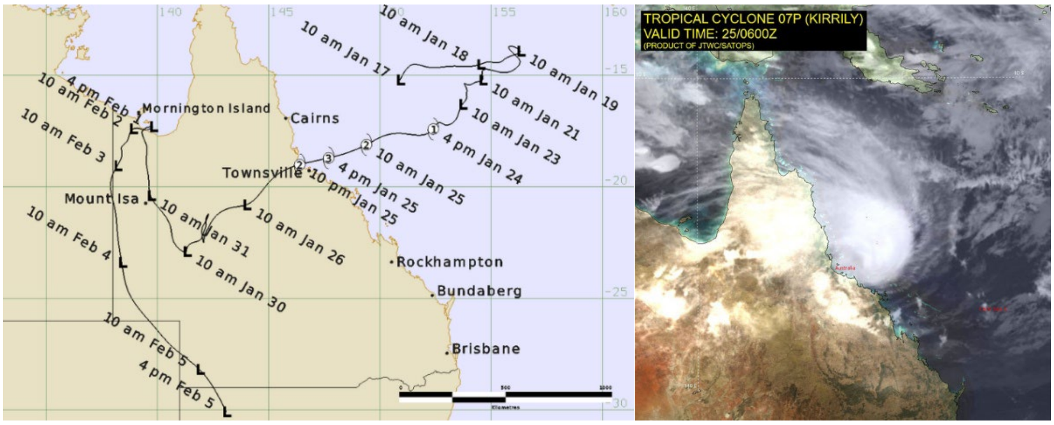

Figure 1: The track of TC Kirrily (from Bureau of Meteorology, http://www.bom.gov.au/cyclone/history/kirrily24.shtml) (left) and the satellite image showing the TC approaching the Queensland coast on 25 January 2024 (right, from NRL, https://www.nrlmry.navy.mil/TC.html).

Severe Tropical Cyclone Kirrily peaked as a Category 3 system in the Coral Sea before crossing the north Queensland coast near Townsville as a Category 1 cyclone (Figure 1). Initially identified as a tropical low (05U) on 17 January 2024, it formed along the monsoon trough and was steered east by strong monsoon winds. By 24 January, it was named Tropical Cyclone Kirrily and began to develop rapidly, reaching peak intensity on 25 January. After crossing the coast, Kirrily moved inland and weakened below tropical cyclone intensity by 26 January. It later moved west and north across Queensland, briefly strengthening over the Gulf of Carpentaria but did not redevelop into a tropical cyclone. Kirrily caused intermittent gales and heavy rainfall, leading to widespread flooding in western Queensland. By 5 February it had merged into an existing trough over southeastern Australia (http://www.bom.gov.au/cyclone/history/kirrily24.shtml).

The ECMWF ERA5 reanalyses (Hersbach et al. 2020) are used to provide a broadscale synoptic setting for TC Kirrily. Figure 2 shows the 850 hPa wind field at 0000 UTC on 18 January 2024 in the early stages of the developing cyclone. The large-scale flow is typical of the Australasian monsoon. There is a band of easterlies between about 5°N and 15°N, which turn to northerlies in the western part of the domain near Singapore, cross the Equator and feed into strong westerlies south of the Equator. The westerlies turn clockwise in the regions of ~135°E and ~160°E, resulting in cyclonic flow and the development of two lows (Figure 2). A few days later the low pressure near ~165ºE became TC Kirrily and the one near ~135°E expanded and deepened to form an almost continental-scale cyclonic circulation.

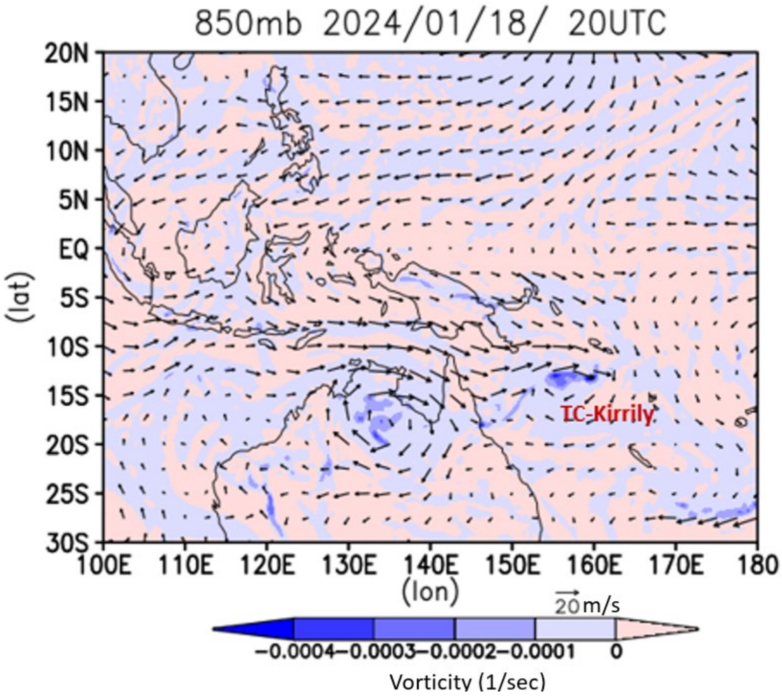

Figure 2: 850 hPa wind vectors (m/s) and vorticity (1/sec) (shaded) from the ERA5 reanalyses at 20 UTC on 18 January 2024 (6:00AM 19 January AEST).

4. Results

4.1. Storm evolution

Figure 3 illustrates the evolution of TC Kirrily in terms of intensity (minimum surface pressure, left panel) and track (right panel) from the model simulations, with the observed best track (Courtney et al., 2020) shown in black. TC Kirrily experienced slow intensification starting on 24 January. This was followed by rapid intensification after 24 hours, reaching a minimum surface pressure of 978 hPa after 36 hours, just before landfall. The cyclone then began to rapidly decay.

In comparison to observations, the default GA8 model (purple line) failed to forecast the rapid intensification of TC Kirrily, predicting a minimum central pressure of 990 hPa (Figure 3, left panel). However, with the CoMorph-A convection scheme, the GA8-CoM model (red line) successfully captured the rapid intensification, reaching a minimum central pressure of 975 hPa after 30 hours, which is slightly deeper and occurs 5 hours earlier than observed (black line). Using the GA9 model (green line), the intensity forecast shows a slight improvement compared to GA8, with the minimum central pressure being about 2-3 hPa deeper. However, it remains weaker than observed and weaker than the GA8-CoM and GA9-CoM (blue line) forecasts. The GA8-CoM and GA9-CoM intensity forecasts are very similar.

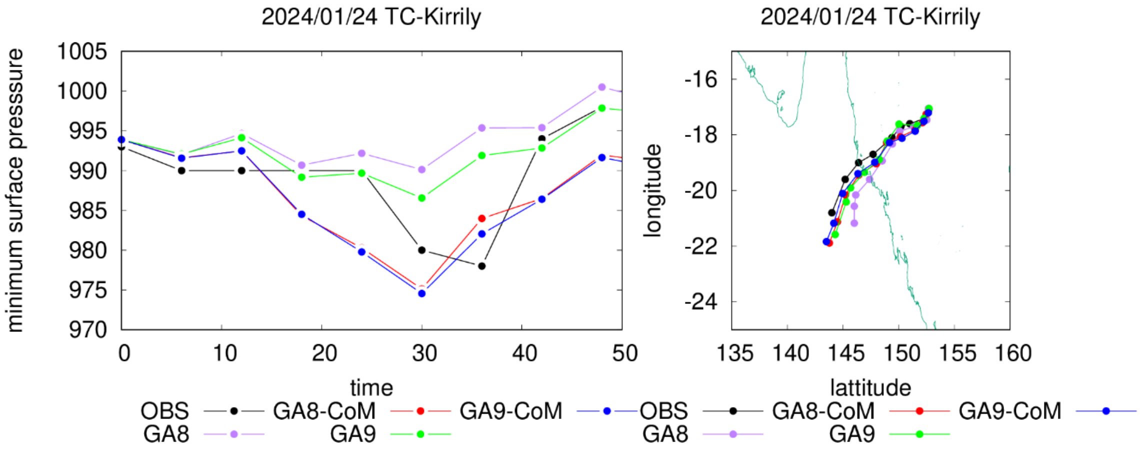

Figure 3:The intensity evolution in terms of minimum surface pressure (left); and the track in terms of the position of the central surface pressure (right) for TC Kirrily from observations (black; the best track database, Courtney et al., 2020) and forecasts from GA8 (purple), GA8-CoM (red) and GA9 (green), and GA9-CoM (blue). The forecasts were initialised at 00UTC on 24th January 2024.

Compared to the observed best track (black line), the track forecasts show a slight southward bias as lead time increases, and the TC nears and moves over land (Figure 3, right panel). This bias is largest in GA8, but in general the tracks from all configurations are very similar.

4.2. Rainfall rate distribution

The modelled total rainfall can be split into the convective rainfall from the convection scheme, representing spatial scales smaller than the grid box, and the large-scale rainfall calculated by the large-scale cloud scheme.

Figure 4 illustrates the total rainfall and the relative contributions of convective and large-scale rainfall from the GA8 model for TC Kirrily at 12, 36 and 48 hours—capturing its development, post-landfall maturity, and decay phases, respectively.

At 12 hours, rainfall is predominantly concentrated within the cyclone's core and along its outer spiral rainbands. The heaviest rainfall is located in the west quadrant of the storm, consistent with its south-westward and cyclonic motion. At this stage, the total rainfall rate is primarily driven by parameterized convection, while large-scale rainfall remains comparatively less and is confined to a smaller region near the storm centre.

At 36- and 48-hours, following landfall, the total rainfall becomes increasingly confined to the cyclone's core, while the outer spiral rainbands weaken substantially. In the GA8 simulation, convective rainfall dominates both the inner core and the outer bands, closely mirroring the spatial distribution of total rainfall. Although the contribution from large-scale rainfall increases compared to earlier developmental stages, it remains relatively lower than that of convective rainfall and is spatially limited—primarily occurring in the TC core region. This distribution underscores the dominant role of parameterized convection in GA8 in driving moisture processes throughout the lifecycle of Tropical Cyclone Kirrily.

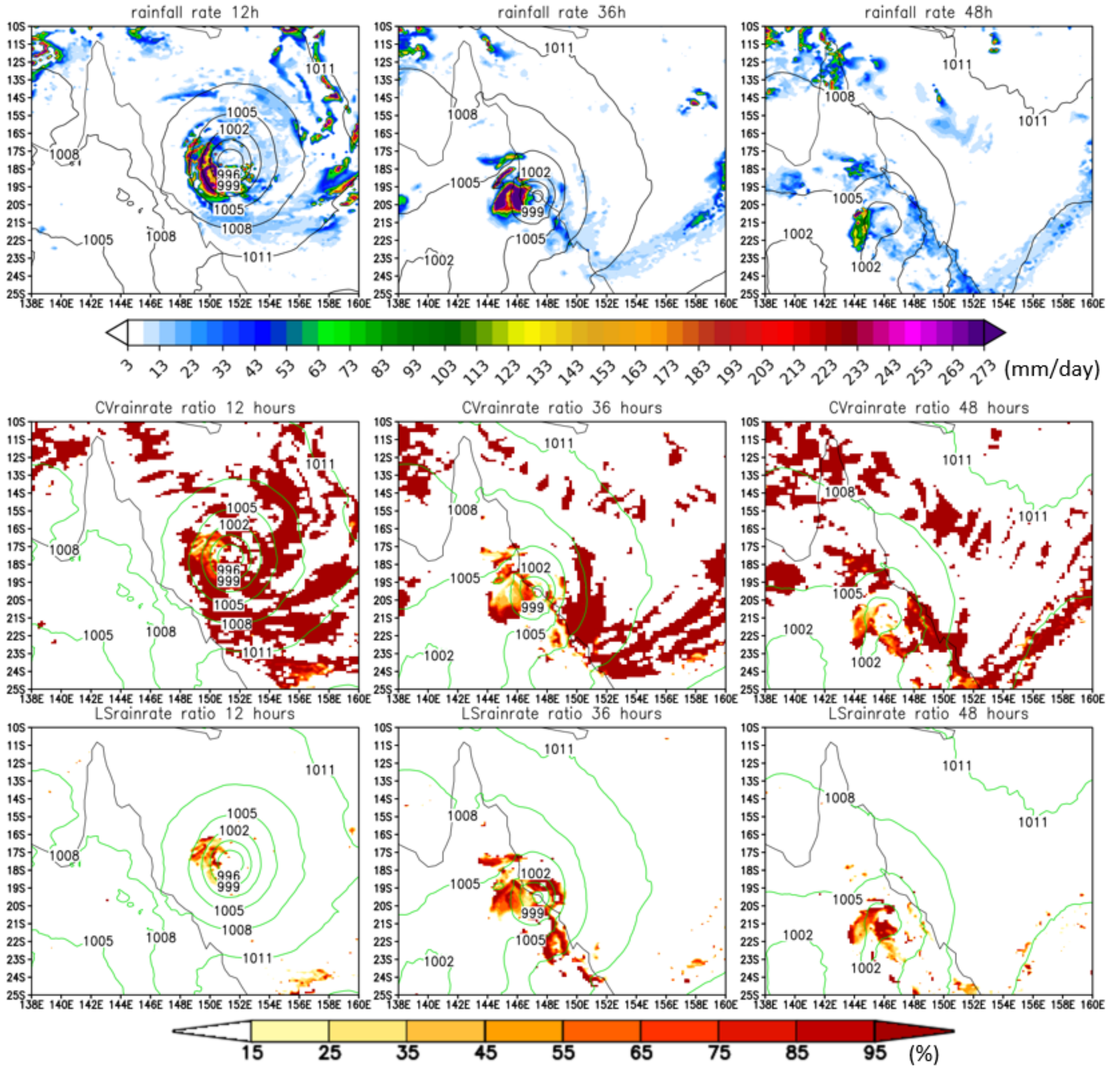

Figure 4: Rainfall rate (mm/day; top row) and the proportion (%) of the total rainfall that is convective (middle row) and large scale (bottom row) rainfall, respectively, from GA8 model forecasts at 12 hours (left column), 36 hours (middle column) and 48 hours (right column). The black contours (top panel) and green contours (the lower two panels) denote the mean sea level pressure (hPa).

Figure 5 presents the corresponding results for the GA8-CoM experiment. Compared to the GA8 simulation (Figure 4), the total rainfall rates in GA8-CoM are notably higher within the cyclone's core region across all three integration times, consistent with the higher storm intensity shown in Figure 3. A key distinction between GA8 and GA8-CoM is the greater proportion and spatial extent of large-scale rainfall with GA8-CoM, which is significantly higher than in the GA8 experiment. In contrast, the convective rainfall contribution is relatively reduced, though still present in the core and outer regions. This indicates that large-scale moisture processes play a more dominant role in the GA8-CoM simulation, contributing to the storm's stronger intensification by enhancing sustained rainfall within the cyclone core.

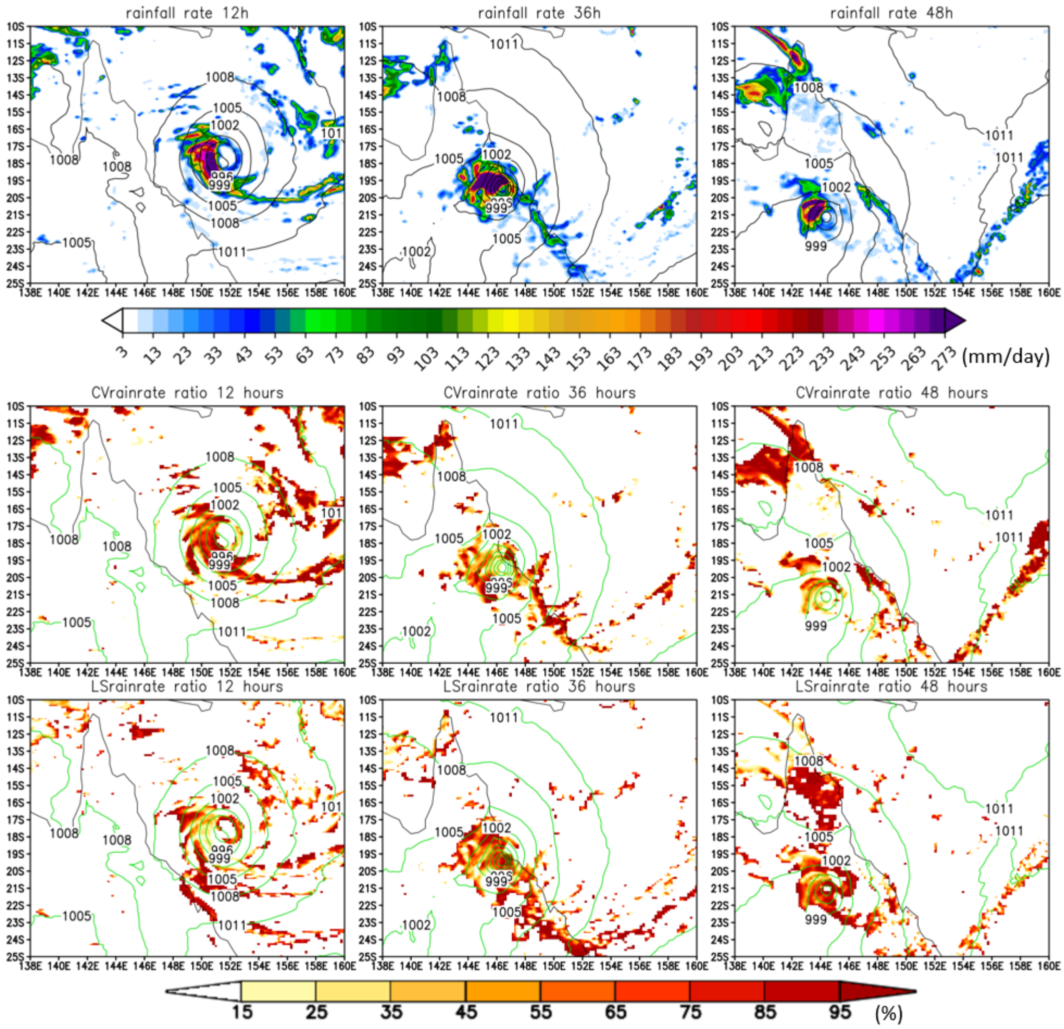

Figure 5: As for Fig. 4, but for the GA8-CoM experiment.

Figure 6 presents the total rainfall rates and the relative contributions of convective and large-scale rainfall from the GA9 forecast. The structure and evolution of rainfall closely resemble those seen in the GA8 simulation (Figure 4). Convective rainfall remains dominant in both the inner core and outer bands, while the proportion of large-scale rainfall is limited in spatial extent, primarily concentrated near the cyclone core region. There is some indication of slightly higher large-scale rainfall proportions in GA9 than in GA8, suggesting an enhanced role of large-scale moisture processes within the cyclone core in GA9. However, the results still indicate that parameterized convection is the primary driver of rainfall throughout TC Kirrily's lifecycle in the GA9 forecast.

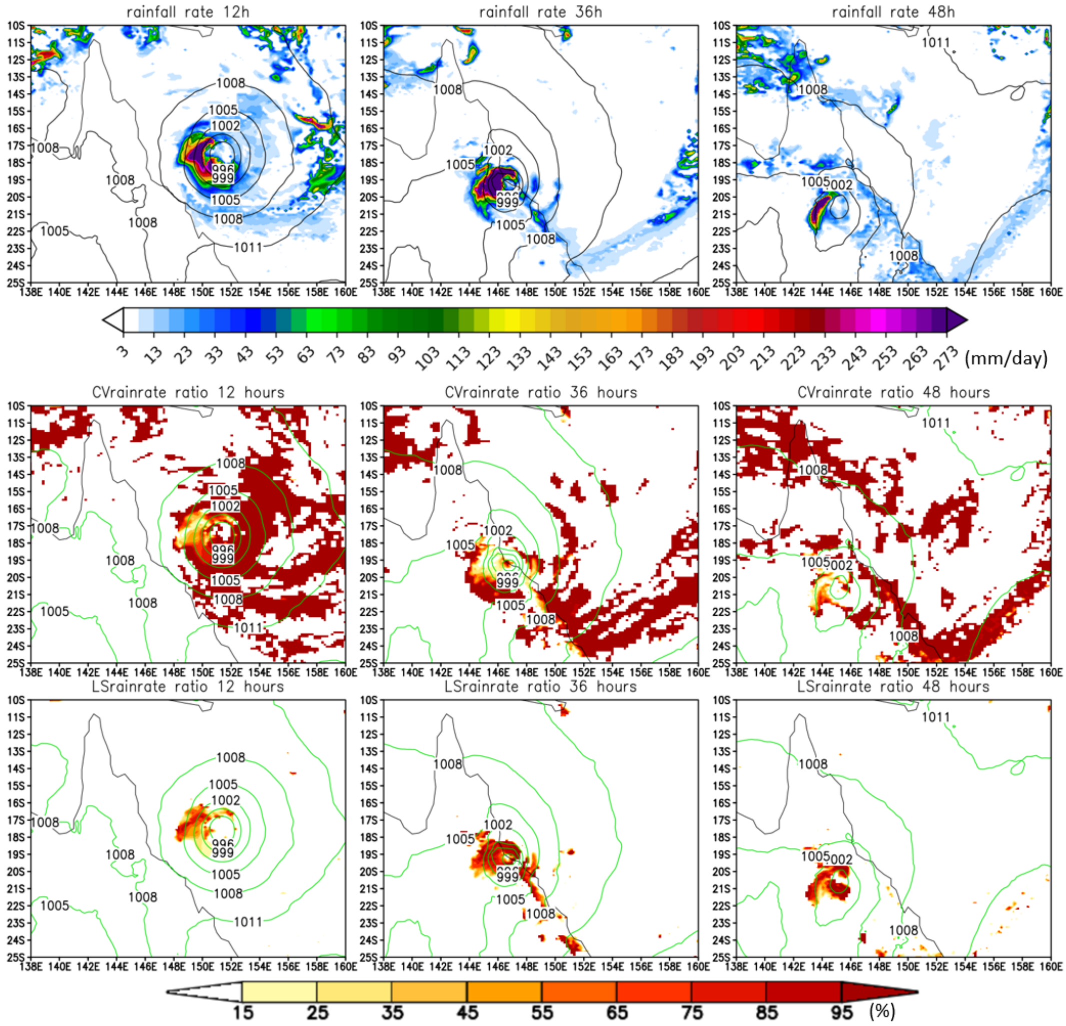

Figure 6: As for Fig. 4, but for the GA9 experiment.

The spatial and temporal results from the GA9-CoM forecast (Figure 7) are very similar to those from the GA8-CoM experiment, indicating similar model behaviour under the CoMorph-A package. Compared to using the default convection scheme in GA8 and GA9, the CoMorph-A package is enhancing large-scale moisture processes, increasing the proportion of large-scale rainfall and contributing to an improvement in the storm's overall structure and intensity as discussed in the following sections.

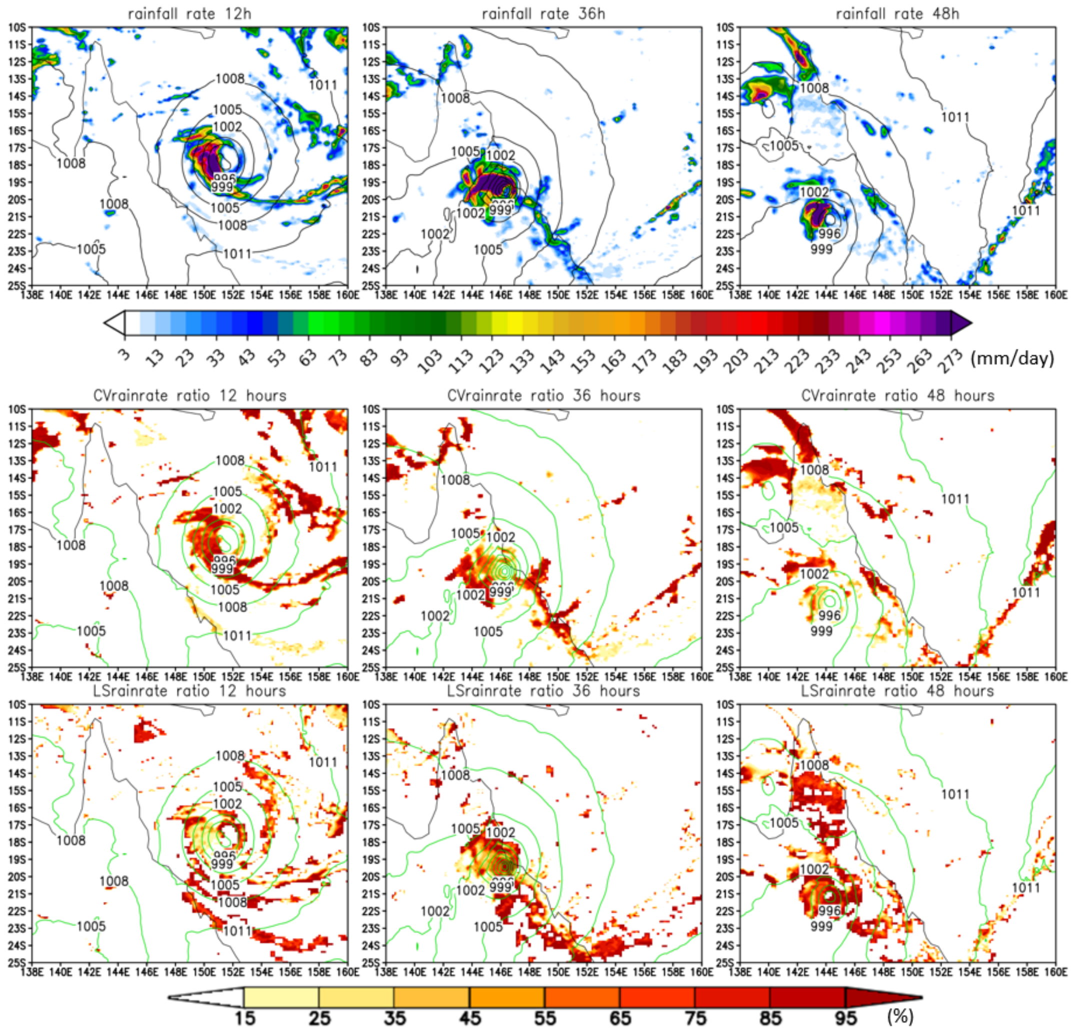

Figure 7: As for Fig. 4, but for the GA9-CoM experiment.

4.3. Azimuthal analysis

4.3.1. Rainfall rate

To better understand the impacts of the convection schemes on the evolution of the TC, we compare time–radius plots of selected azimuthally averaged model quantities.

Figure 8 presents time–radius plots of the convective and large-scale rainfall rates respectively, azimuthally averaged around the TC centre, in the forecasts with GA8 and GA8-CoM. The y-axis shows the time evolution of the forecast.

In the GA8 forecast, the azimuthally averaged convective rainfall (Figure 8c) dominates during the TC intensification period (about 0-30h), primarily located beyond a 120 km radius from the centre of the cyclone. It reaches a maximum of ~90 mm/day at around 120 km at 20 hours of integration, after which the convective rainfall rapidly dissipates. The large-scale rainfall in GA8 (Figure 8a) is negligible in the early hours of integration, reaching a maximum value of ~30 mm/day around 20 hours, when the storm reaches its maximum intensity (Figure 3) and then dissipates outward.

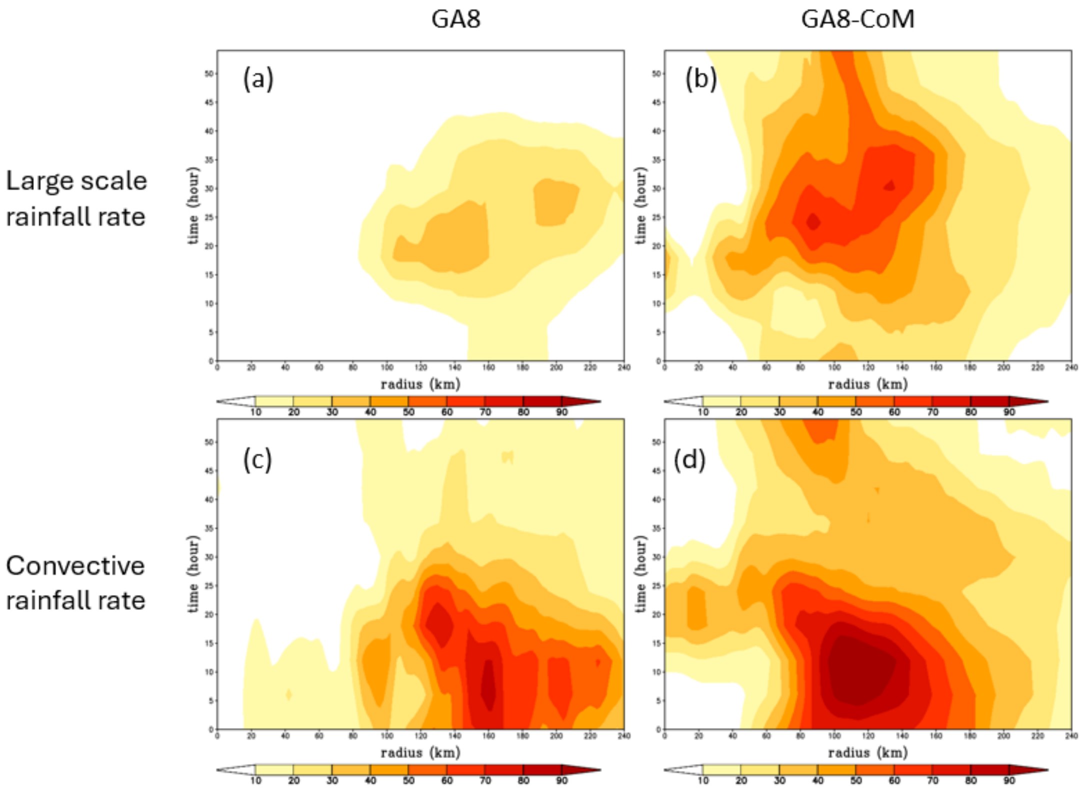

Figure 8: Time-radius plots of the azimuthal average of the large-scale (a and b) and convective (c and d) rainfall rates (mm/day) respectively for the GA8 experiment (left) and GA8-CoM experiment (right).

For the GA8-CoM forecast, similar to the GA8 results, convective rainfall (Figure 8d) dominates during the TC's developing and intensifying periods, while large-scale rainfall (Figure 8b) becomes more significant when the TC reaches its mature stage. However, the azimuthally averaged convective rainfall moves inward, reaching a maximum value of ~140 mm/day at 15 hours of integration and continues to move inward around 20 hours of integration (Figure 8d). Subsequently, the convective rainfall decreases rapidly but still remains active in the TC core region (around a 100 km radius). The convective rainfall rate structure in the GA8-CoM experiment (Figure 8d) is much smoother compared to the GA8 experiment (Figure 8c). The large-scale rainfall in GA8-CoM (Figure 8c) gradually increases with TC intensification, reaching a maximum value of ~90 mm/day at a radius of 80 km when the TC reaches its maximum intensity, and thereafter it remains dominant over the convective rainfall in the TC core region.

One important difference between GA8 and GA8-CoM is the dominant role of large-scale rainfall beyond integration 20h of the TC in GA8-CoM (Figure 8). In GA8-CoM, the large-scale rainfall emerges and reaches its maximum leading up to the mature stage of the TC and is maintained in the core region. This sustained convection drives strong upward motion within the TC core, maintain the secondary circulation of the cyclone (Zhu et.al.

2001) Consequently, TC-Kirrily undergoes the rapid intensification and reaches its mature stage. In contrast, the large-scale rainfall in GA8 fails to reach an intensity comparable to the convective rainfall and does not become dominant in the core region. As a result, the vertical motion in the core region is much weaker and dissipates quickly above the boundary layer (Fig.9 a,c), and the simulated tropical cyclone fails to rapidly intensify and reaches its mature stage.

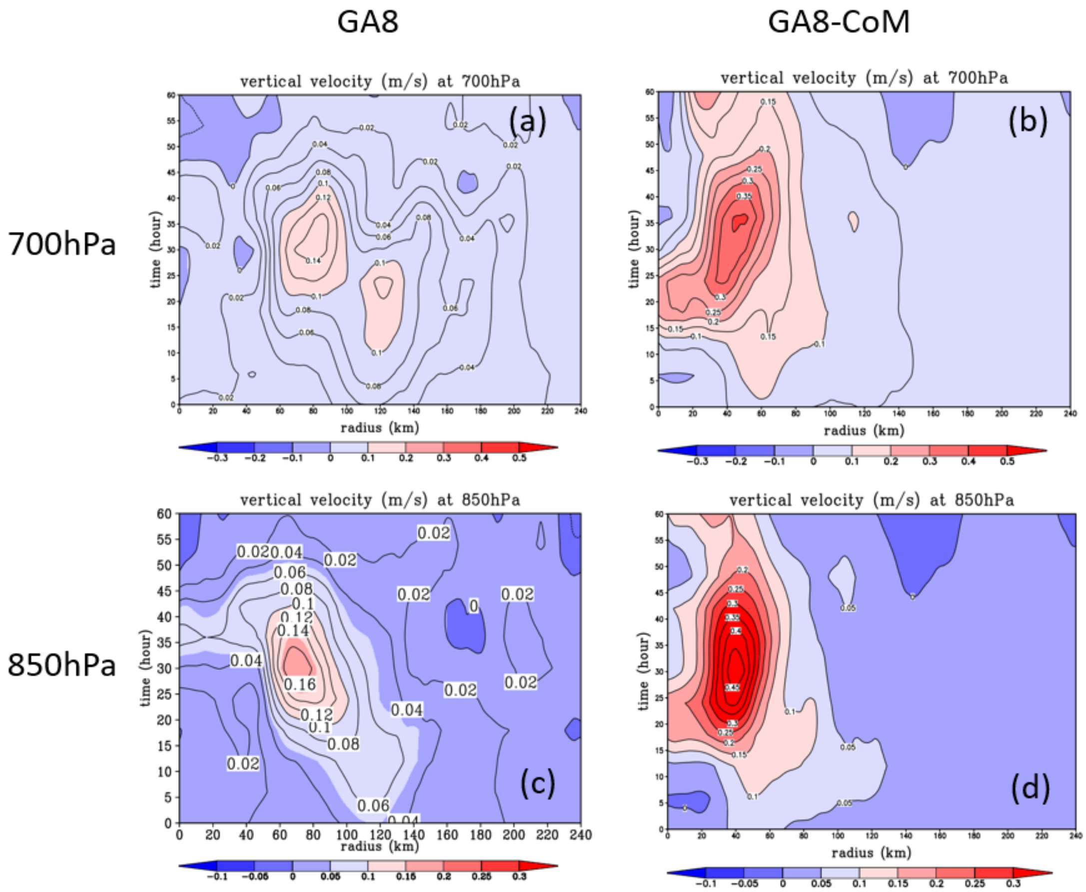

Figure 9: Time-radius plots of the azimuthal average of the vertical motion at 700hPa (a and b) and 850hPa (c and d) respectively for the GA8 experiment (a,c) and GA8-CoM experiment (b,d).

Figure 10a and c present time–radius plots of azimuthally averaged rainfall rates from the GA9 simulation. The results show that convective rainfall dominates during the early development and intensification phases of the cyclone, with peak values occurring around 140 km from the centre. This convective activity begins to weaken after ~15-20 hours of integration. In contrast, large-scale rainfall intensifies rapidly around the same radial distance, peaking between ~25- 30 hours, followed by outward propagation and rapid decay.

Compared to the GA8 simulation, the large-scale rainfall in GA9 is significantly stronger and more persistent, contributing to its stronger intensification (Figure 3a). However, the large-scale rainfall in GA9 doesn't persist for as long as in the GA9-CoM simulation (Figures 10a, b), and its peak is located slightly farther from the cyclone centre.

The GA9-CoM simulation exhibits patterns similar to GA8-CoM, with enhanced large-scale rainfall concentrated in the TC core region during the rapid intensification and mature stages. This behaviour underscores the role of the CoMorph-A convection package in strengthening large-scale moisture processes and promoting more organized and intense tropical cyclone development.

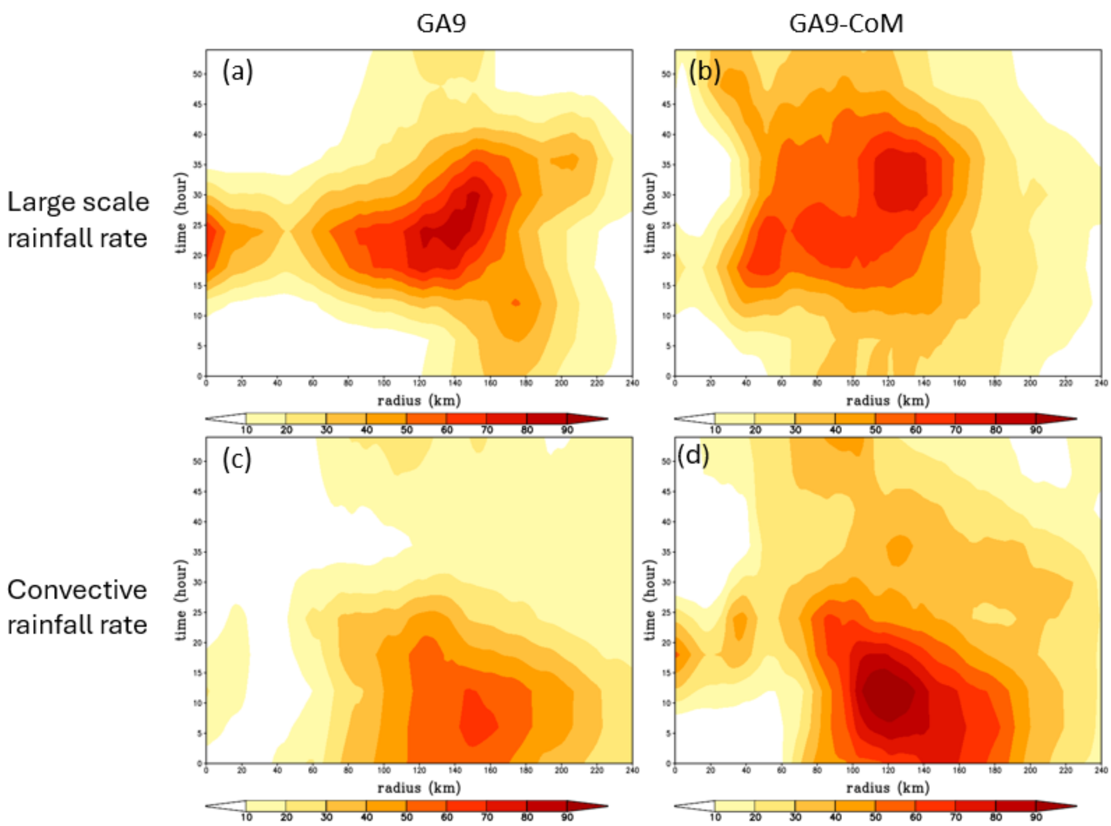

Figure 10: As for Fig. 8, but for GA9 and GA9-CoM.

The transition from convective to large-scale rainfall in GA8-CoM and GA9-CoM that is seen during the life-cycle of the TC is consistent with the results of Zhu et al. (2001), who examined explicit and parameterised representations of moist processes using a TC model. In their results, during the early stages of evolution, precipitation is wholly associated with the convection scheme. However, as grid-scale saturation occurs, the parameterization scheme's contribution decreases rapidly, marking the beginning of the rapid deepening period. Subsequently, precipitation occurs predominantly on the grid scale. A similar finding is discussed in Baik et al. (1990), who used the Betts–Miller parameterization scheme in an axisymmetric model with 11 vertical levels. They show that the TC rapid intensification coincides with a sharp increase in grid-scale precipitation and a decline in subgrid-scale precipitation.

Majumdar et al. (2023) present forecasts of convective and large-scale rainfall rates associated with TC Laura using the 4-km global ECMWF model (EC4). Their analysis reveals that at 60 hours into the simulation—corresponding to the cyclone's peak intensity—rainfall within the core region was predominantly driven by large-scale processes (see their Fig. 6e). In contrast, convective rainfall was relatively weak and primarily confined to the spiral rainbands outside the core (see Fig. 6b). However, their study does not address the evolving roles of convective and large-scale rainfall processes throughout the different developmental stages of the tropical cyclone.

4.3.2. Relative humidity and wind

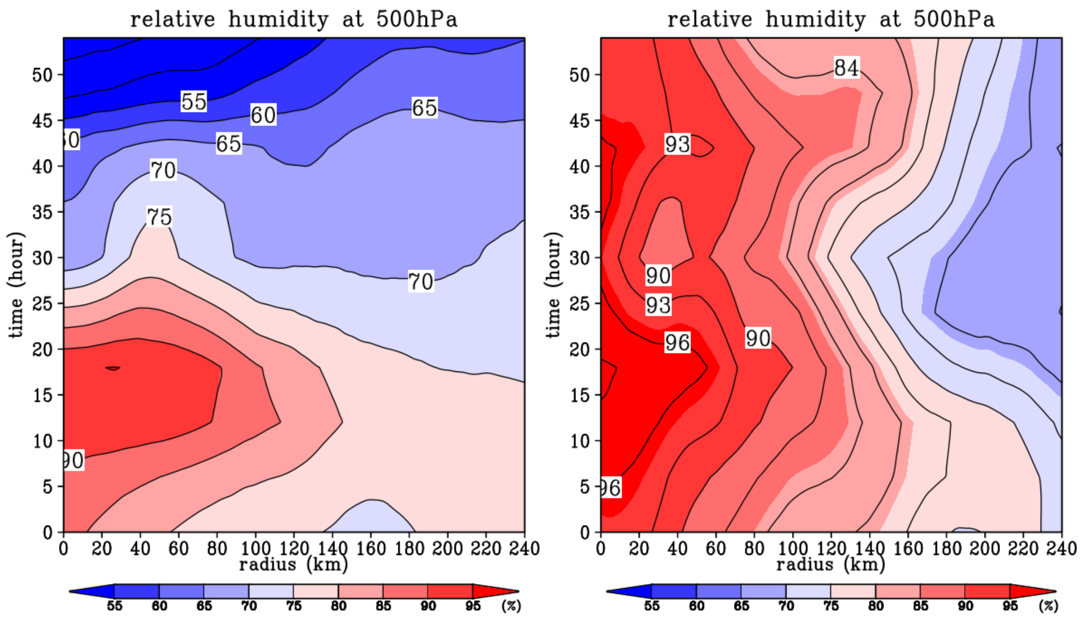

Figure 11: Time-radius plots of the azimuthal averaged relative humidity at 500hPa for GA8 (left) and GA8-CoM (right).

The distribution of convective and large-scale rainfall significantly impacts the moisture and temperature distribution of TCs. Figure 11 illustrates the azimuthally averaged 500 hPa relative humidity relative to the TC centre. In the GA8 simulation, parametrized convection dominates during the TC development period. Increased subgrid-scale convection raises the relative humidity in the TC core region, reaching a maximum value of over 90% around 18 hours into the integration, indicating a stage of quasi-saturation. When the TC reaches quasi-saturation in the core, subgrid convection rapidly decreases (Figure 8c). Due to the lack of large-scale rainfall in the TC core region when convective rainfall decreases, the moisture in the core region beyond 20 hours of integration fails to maintain a quasi-saturation state and dries out rapidly, dropping below 60%. Consistent with the moisture distribution in the left panel of Figure 10, the azimuthal wind at 850 hPa in left panel of Figure 12 shows increased inward movement of horizontal wind, reaching a maximum value of ~26 m/s at a radius of 120 km around 23 hours into the integration, driven by increased subgrid convection. After 23 hours integration, the azimuthally averaged wind weakens outward because the TC fails to maintain a quasi-saturated core without large-scale rainfall being triggered in the core.

In the GA8-CoM forecast, the TC core region experiences increased relative humidity during the developing period due to rising subgrid-scale convection, similar to GA8. Subsequently, large-scale rainfall peaks and sustains in the core region during the rapid intensification and mature stages of the TC, while convective rainfall rapidly decreases. As a result, the TC core region within 120 km in GA8-CoM maintains a moist static state with more than 90% saturation up to 60 hours of integration. As shown in Figure 8b, the large-scale rainfall reaches its maximum in the core around 30 hours, leading to the quasi-saturation of the core during the TC's rapid intensification and mature stages. The strong heat release from the large-scale moisture process drives strong inward motion of the wind close to the TC centre and maintains the small radius of the maximum azimuthal wind for a lasting period during the mature stage of TC Kirrily (left panel of Figure 12). The strongest azimuthally averaged winds at 850 hPa move inward during the TC developing stage, similar to GA8, reaching a maximum value of 36 m/s at a radius of 60 km. The winds are therefore significantly stronger (36 m/s versus 26 m/s) and closer to the TC centre (60km versus 120km) than seen with GA8, and the strong winds are maintained in the core region for a significantly longer period of time (Figure 12).

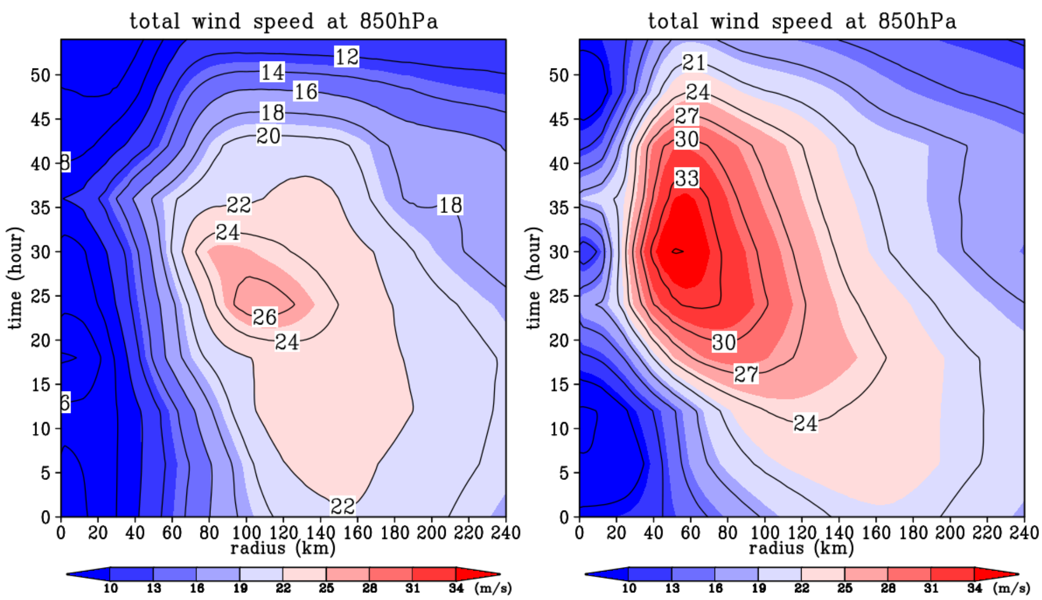

Figure 12: Time-radius plots of azimuthal average of the total wind speed (m/s) at 850hPa for GA8 (left) and GA8-CoM (right).

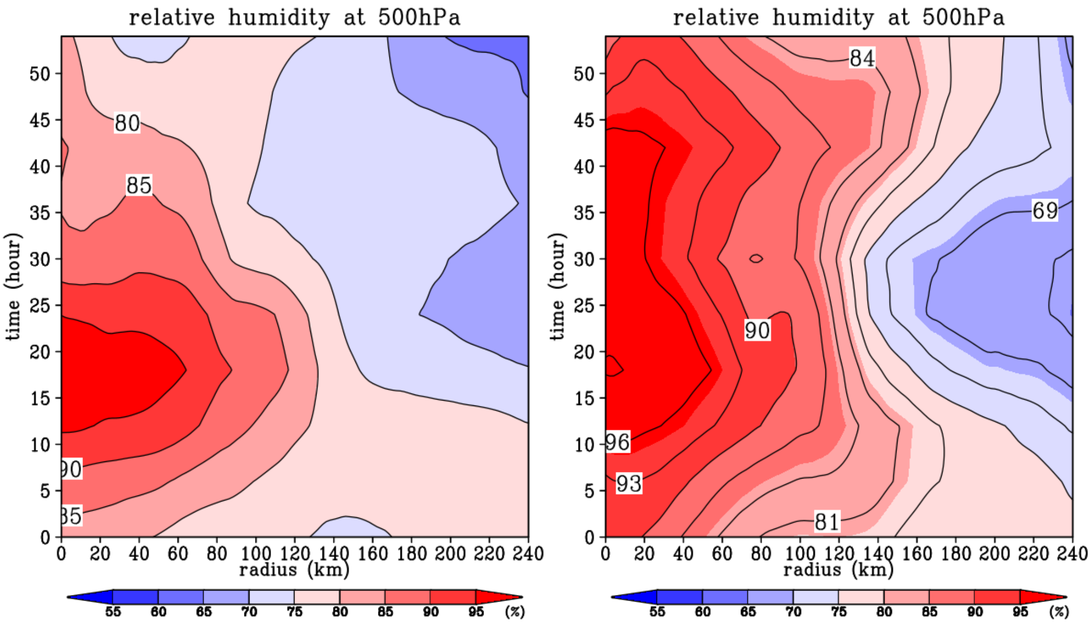

Figure 13: As for Figure 10, but for GA9 (left) and GA9-CoM (right).

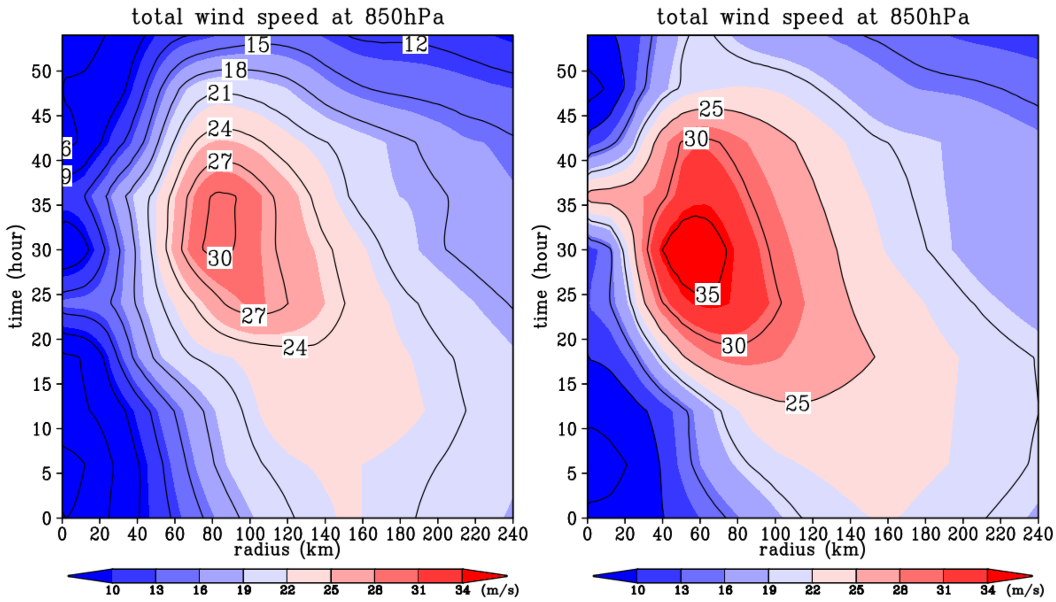

Figure 14: As for Figure 12, but for GA9 (left) and GA9-CoM (right).

Figures 13 and 14 show the respective relative humidity and wind speed plots for the GA9 and GA9-CoM simulations. Due to the enhanced role of large-scale moisture processes in the GA9 configuration (Figure 10) compared to GA8 (Figure 8), the core region of the TC maintains elevated relative humidity levels (above 70%) during its mature stage in GA9 (left panel of Figure 13). Correspondingly, the maximum azimuthal wind speed in GA9 reaches a higher intensity of 28 m/s and is located closer to the cyclone centre (approximately 90 km in radius) (left panel of Figure 14) compared to the GA8 simulation (left panel of Figure 12).

With the CoMorph convection scheme, the GA9-CoM simulation exhibits similar characteristics in azimuthally averaged relative humidity and wind fields (right panels of Figures 13, 14) to GA8-CoM (right panels of Figures 11, 12). These results further support the conclusion that the CoMorph scheme promotes a more organized and intensified circulation structure within the cyclone.

5. Discussion and conclusions

Tropical Cyclone Kirrily formed on January 17, 2024, intensified into a Category 3 cyclone, and eventually weakened after making landfall. This study examines the impact of CoMorph-A on forecasts of TC Kirrily using the Unified Model (UM) GA8 and GA9 models.

The results indicate that GA8 struggled to capture the cyclone’s rapid intensification, leading to discrepancies in its predicted evolution and intensity. In contrast, GA8-CoM demonstrated a significant improvement, better replicating Kirrily’s evolution.

A key difference between the two configurations lies in the coupling of convective and large-scale rainfall. The default GA8 model captures the dominant role of parameterized convective rainfall during the developing stage of the cyclone. However, as this component rapidly decreases in the cyclone's core when the moist static stage is reached, large-scale rainfall fails to dominate. Consequently, the core region fails to keep ascending motion and dries out above the boundary layer, leading to a weakening of the storm’s structure and wind strength. In contrast, GA8-CoM captures the transition in the character of deep convection in the inner core region from being driven by parameterized convection to being driven by large-scale moisture processes. This transition maintains the secondary circulation, drives the rapid intensification and helps maintain the cyclone’s strength.

Using GA9, the contribution of large-scale rainfall is enhanced compared to GA8, which leads to a slight improvement in terms of the intensity forecast for TC-Kirrily, but convective processes still dominate. The improvement of GA9 over GA8, such that it starts to more closely resemble the simulations using CoMorph-A, may be due to the inclusion of modifications to the other parameterisation schemes within the CoMorph-A package in GA9 (albeit not the convection scheme itself) in addition to the updates to the convection scheme. The GA9-CoM simulation exhibits very similar characteristics in the contributions of convective and large-scale moisture processes, as well as in azimuthally averaged humidity and wind fields, as the GA8-CoM simulation.

Similar results were observed for TC Alfred, which occurred in March 2025. However, for tropical cyclones that develop a strongly asymmetric structure, the azimuthal-mean analysis used in this study may not be applicable. The findings of this study underscore the critical role of advanced convection schemes like CoMorph in numerical weather prediction models. By improving the representation of interactions between convection and large-scale atmospheric processes, such schemes enhance the accuracy of tropical cyclone forecasts, ultimately supporting more effective disaster preparedness and risk mitigation efforts. The combined influence of convective and large-scale moisture processes on tropical cyclone development remains underexplored in current forecast models. The methodology employed in this study offers a valuable framework for evaluating and improving the performance of convection parameterization for TC forecasts.

Acknowledgements

Ac SLL is funded by Meat and Livestock Australia, the Queensland Government through the Drought and Climate Adaptation Program, and the University of Southern Queensland through the Northern Australian Climate Program (NACP). The authors thank Bethan White and Shaun Cooper for their constructive feedback on the manuscript.

References

Arakawa A., 2004: The cumulus parameterization problem: past, present, and future. J Clim 17(13):2493–525. https://doi.org/10.1175/1520-0442(2004)017<2493:RATCPP>2.0.CO;2.

Betts, A. K., 1997: Parameterisation of deep convection. *The physics and parameterization of moisture atmospheric convection (Ed. R.K.Smith), Kluwer, Dorecht, 255-279*

Baik, J.-J., & Paegle, J. (1990). Effects of cumulus convection on the barotropic instability of the tropical easterly jet. Journal of the Atmospheric Sciences, 47(1), 77-90.

Courtney, J. B. et al. Towards an objective Tropical Cyclone dataset for the Australian region. Trop. Cyclone Res. 9, 23–36 (2020).

Ma, L. M., Z. Tan, 2009: Improving the behavior of the cumulus parameterization for tropical cyclone prediction convection trigger. *Atmos Res* 92:190–211. https://doi.org/10.1016/j.atmosres.2008.09.022

Majumdar, S. J, L. Magnusson, P. Bechtold and J. Bidlot, 2023: Advanced Tropical Cyclone Prediction Using the Experimental Global ECMWF and Operational Regional COAMPS-TC Systems, *Mon. Wea. Rev. 2029-2048, https://doi.org/10.1175/MWR-D-22-0236.1*

Lavender, S., Stirling, A.J., Whitall, M., Stratton, R.A., Daleu, C.L., Plant, R.S., Lock A. 2024, The use of idealised experiments in testing a new convective parameterization: Performance of CoMorph-A-A, *Quart. J. Roy. Meteor. Soc.*, 10.1002/qj.4660

Lock, A., Whitall, M., Stirling, A.J, Williams, K., Lavender, S., Stratton, R.A., 2024: The performance of the CoMorph-A-A convection package in global simulations with the Met Office Unified Model, *Quart. J. Roy. Meteor. Soc.*, doi:10.1002/qj.4781

Shen, W., Song, J., Liu, G. et al., 2019: The effect of convection scheme on tropical cyclones simulations over the CORDEX East Asia domain. *Clim Dyn* 52, 4695–4713. https://doi.org/10.1007/s00382-018-4405-y

Smith, K. R., 2000: The role of cumulus convection in hurricane models. *Rev. Geophys*. 38, 465-489

Shepherd, T. J., K. J. Walsh, 2016: Sensitivity of hurricane track to cumulus parameterization schemes in the WRF model for three intense tropical cyclones: Impact of convective asymmetry. Meteorol Atmos Phys. https://doi.org/10.1007/s00703-016-0472-y

Whitall M, Matsubayashi K (2022) The CoMorph-A convection scheme.UM Documentation Paper 043, UK Met Office

Willett, M. R., Brooks, M., Bushell, A., Earnshaw, P., Smith, S., Tomassini, L., Best, M., Boutle, I., Brooke, J., Edwards, J. M., Furtado, K., Hardacre, C., Hartley, A. J., Hewitt, A., Johnson, B., Lock, A., Malcolm, A., Mulcahy, J., Müller, E., Rumbold, H., Rooney, G. G., Sellar, A., Ujiie, M., van Niekerk, A., Wiltshire, A., and Whitall, M.: The Met Office Unified Model Global Atmosphere 8.0 and JULES Global Land 9.0 configurations, EGUsphere [preprint], https://doi.org/10.5194/egusphere-2025-1829, 2025.

Xavier, P., co-authors: Assessment of the Met Office Global Coupled model version 5 (GC5) configurations (2023). Met Office report.

Zhu. H, R. Smith and W. Ulrich, 2001: A minimal three-dimensional tropical cyclone model, *J. Atmos, Sci.,* 58, 1924-1444.

Zhu H et al., 2024: Impacts of the new UM convection scheme, CoMorph-A,over the Indo-Pacific and Australian regions. *Journal of Southern Hemisphere Earth Systems Science*, 74, ES23011.doi:10.1071/ES23011

MJ Zidikheri, PJ Steinle, Y Xiao, EA Villardon, 2024: An objective evaluation of the Bureau's ACCESS-GE4 global ensemble model, Mon. Wea. Rev, 137, 1717-1720.